1   **The Fertilizing Role of African Dust in the Amazon Rainforest: A First**

2   **Multiyear Assessment Based on CALIPSO Lidar Observations**

3

4   Hongbin Yu[1,2], Mian Chin[2], Tianle Yuan[2,3], Huisheng Bian[2,3], Lorraine A. Remer[3],

5   Joseph M. Prospero[4], Ali Omar[5], David Winker[5], Yuekui Yang[2,6], Yan Zhang[2,6], Zhibo

6   Zhang[7], Chun Zhao[8]

7

8   [1] Earth System Science Interdisciplinary Center, University of Maryland, College Park,
9   Maryland, USA

10   [2] Earth Sciences Division, NASA Goddard Space Flight Center, Greenbelt, Maryland,
11   USA

12   [3] Joint Center for Earth Science and Technology, University of Maryland at Baltimore
13   County, Baltimore, Maryland, USA

14   [4] Cooperative Institute for Marine and Atmospheric Studies, Rosenstiel School of Marine
15   and Atmospheric Science, University of Miami, Miami, Florida, USA

16   [5] NASA Langley Research Center, Hampton, Virginia, USA

17   [6] Universities Space Research Association, Columbia, Maryland, USA

18   [7] Department of Physics, University of Maryland at Baltimore County, Baltimore,
19   Maryland, USA

20   [8] Atmospheric Science and Global Change Division, Pacific Northwest National
21   Laboratory, Richland, Washington, USA

22   ***Correspondence***
23   Hongbin Yu

24   NASA GSFC Code 613

25   Greenbelt, Maryland 20771

26   Hongbin.Yu@nasa.gov

27   301-614-6209

28

31

32

33   **Abstract**: The productivity of the Amazon rainforest is constrained by the availability of

34   nutrients, in particular phosphorus (P). Deposition of long-range transported African dust

35   is recognized as a potentially important but poorly quantified source of phosphorus. This

36   study provides a first multiyear satellite-based estimate of dust deposition into the

37   Amazon Basin using three dimensional (3D) aerosol measurements over 2007-2013 from

38   the Cloud-Aerosol Lidar with Orthogonal Polarization (CALIOP). The 7-year average of

39   dust deposition into the Amazon Basin is estimated to be 28 (8~48) Tg a^{-1} or 29 (8~50)

40   kg ha^{-1} a^{-1}. The dust deposition shows significant interannual variation that is negatively

41   correlated with the prior-year rainfall in the Sahel. The CALIOP-based multi-year mean

42   estimate of dust deposition matches better with estimates from in-situ measurements and

43   model simulations than a previous satellite-based estimate does. The closer agreement

44   benefits from a more realistic geographic definition of the Amazon Basin and inclusion

45   of meridional dust transport calculation in addition to the 3D nature of CALIOP aerosol

46   measurements. The imported dust could provide about 0.022 (0.006~0.037) Tg P of

47   phosphorus per year, equivalent to 23 (7~39) g P ha^{-1} a^{-1} to fertilize the Amazon

48   rainforest. This out-of-Basin P input largely compensates the hydrological loss of P from

49   the Basin, suggesting an important role of African dust in preventing phosphorus

50   depletion on time scales of decades to centuries.

51

1.   Introduction

The Amazon rainforest represents about half of the planet's remaining rainforests and is an important ecosystem that plays a crucial role in regulating the Earth's climate. Relatively small changes in the forest cover and productivity could have important implications for the carbon cycle, atmospheric circulations, the hydrology cycle, and climate from regional to global scales *[Shukla et al., 1990; Nepstad et al., 2008; Malhi et al., 2008]*. Phosphorus (P) is the principal fertility factor influencing tree growth across the Amazon Basin *[Vitousek, 1984; Mercado et al., 2011]*. However, 90% of soils in the Amazon Basin are P-deficient *[Sanchez et al., 1982]*. It has been suggested that long-term productivity of the Amazon rainforest depends highly on the atmospheric deposition of dust that may come from a distant ecosystem such as the Saharan desert *[Okin et al., 2004]*. Although the presence of African dust in the Amazon Basin has long been observed *(Artaxo et al., 1990; Talbot et al., 1990; Formenti et al., 2001; Schafer et al., 2008; Ansmann et al., 2009; Ben-Ami et al., 2010; Baars et al., 2011, 2012)*, the dust deposition and associated P input are not yet well quantified. Recently, advanced satellite observations with routine sampling and large spatial and temporal coverage have become ideal for quantifying the inter-continental transport and deposition of aerosol *[Kaufman et al., 2005; Yu et al., 2008, 2012a, 2013]*. Substantial discrepancies still exist between measurements and models *[e.g., Swap et al., 1992 or S92; Kaufman et al., 2005 or K05; Bristow et al., 2010; Ridley et al., 2012]*.

Factors contributing to the large discrepancies in the dust deposition are not fully understood or at least not adequately accounted for. There are several possible reasons for

75   the large range of discrepancy between the different estimates of dust deposition into the

76   Amazon Basin. First, each individual estimate is subject to specific uncertainties, some

77   large.   In addition, the inter-comparisons have often been complicated by issues such as

78   differences in geographical definition of the Amazon Basin, year of the assessment, and

79   inclusion or exclusion of meridional transport.

80

81   The main objective of this study is to resolve the previous discrepancies and provide an

82   alternative satellite-based estimate of dust deposition and phosphorus input into the

83   Amazon Basin. We base our estimate on 3D distributions of aerosols from Cloud-Aerosol

84   Lidar with Orthogonal Polarization (CALIOP) onboard the Cloud-Aerosol Lidar and

85   Infrared Pathfinder Satellite Observations (CALIPSO) from 2007 to 2013. Since June

86   2006, CALIOP has been measuring 3D distributions of backscatter/extinction and

87   depolarization ratio of both clear-sky aerosol and above-cloud aerosol over nearly global

88   scale *[Winker et al., 2013; Yu et al., 2012b; Yu and Zhang, 2013; Liu et al., 2014]*. The

89   previous standard for satellite estimates of dust deposition used the MODerate resolution

90   Imaging Spectroradiometer (MODIS) that provides only a 2-dimensional view of the

91   transport *[K05]*. By using 3D measurements from CALIOP, the MODIS uncertainties

92   can be reassessed or reduced. Another improvement over the single-year K05 study is the

93   use of a multi-year data set. We also improve the dust deposition estimate by accounting

94   for both zonal and meridional transport and defining the geographical region of the

95   Amazon Basin more realistically. Note that K05 neglected the meridional transport and

96   included deposition into the nearby ocean by defining their domain as a rectangle. Both

97   simplifications will introduce significant discrepancies in the estimates of seasonal and

4

98   annual dust deposition into the Amazon Basin, and require clarification to resolve the

99   ambiguity and inconsistency in model-observation comparisons and the role of African

100   dust in the biogeochemical cycle of the Amazon.

101

102   **2.   Methodology**

103   We define the Amazon Basin as a region between 12°S and 8°N in latitude and between

104   75°W and 40°W (for the 12°S-2°S latitudinal segment) or 50°W (for the 2°S-8°N

105   latitudinal segment) in longitude, as illustrated in Figure 1 (i.e., the red-line boundaries)**.**

106   The total area of the region is about 9.6 x 10^8 hectares (ha). This definition attempts to

107   cover the major part of the Amazon Basin, while excluding the nearby ocean in the

108   analysis, and without introducing too much complexity. We estimate the meridional dust

109   mass flux at the latitudinal cross sections and the zonal flux at the longitudinal cross

110   sections by using CALIOP measurements of the 3D distribution of aerosol

111   backscatter/extinction and depolarization at 532 nm (version 3, level 2) in both clear sky

112   and above cloud conditions. The dust mass flux in all-sky conditions was calculated as a

113   weighted average of clear-sky and above cloud dust mass flux with respective fraction of

114   occurrence. While details of calculating dust mass fluxes with CALIOP measurements

115   are described in *Yu et al. [2015] (referred to as Y15),* a brief overview of the approach is

116   given as follows.

117

118   We use CALIOP nighttime, high-quality data only, and separate dust from non-dust

119   aerosol by using the CALIOP depolarization ratio (δ) measurements with *a priori*

120   knowledge of characteristic depolarization ratios for dust and non-dust particles. There is

121   a range of δ values associated with dust and non-dust aerosol. As discussed in Y15, we

122   bound the range of dust fraction introduced by variability in δ and use an average of dust

123   mass fluxes between the upper and lower bounds to represent the best estimate of dust

124   transport and deposition. The difference between the best estimate and the bounds

125   represents an uncertainty associated with the dust discrimination. The CALIOP-based

126   estimate of dust mass flux is also subject to uncertainties associated with CALIOP

127   extinction, vertical profile shape, dust mass extinction efficiency, and possible change of

128   dust size distribution during the transport. The cumulative uncertainty of all these error

129   sources has been estimated to be ±70%, near South America and the Caribbean Sea

130   *[Y15]*. Additional uncertainty may arise from the below-cloud dust missed by CALIOP

131   and possible diurnal variations of dust transport, which however cannot be quantified

132   because of the lack of reliable observations *[Y15]*.

133

134   Dust transport and deposition to the Amazon Basin is predominated by the trans-Atlantic

135   transport in the northeasterly trade winds during boreal winter (December-January-

136   February or DJF) and spring (March-April-May or MAM) *[Prospero et al., 1981; S92;*

137   *Prospero et al., 2014]*. In boreal summer and fall when the Intertropical Convergence

138   Zone moves northward, the majority of dust is transported by the easterly trade winds to

139   the Caribbean Sea and North America *[Prospero et al., 1981; Prospero et al., 2014]*. Our

140   analysis of CALIOP observations derives the 7-year average dust deposition into the

141   Amazon of -0.22 Tg (ranging from -1.51 to +1.97 Tg) in boreal summer and fall. The

142   negative deposition fluxes are not physical and could have resulted from a differentiation

143   of small fluxes at the boundaries of the Amazon Basin. Thus we assume the dust

144   deposition into the Amazon Basin is negligible in boreal summer and fall, similar to S92.

145   Subsequent discussion will be focused on the dust deposition in DJF and MAM.

146

147   **3.   Results and Discussion**

148   **3.1.   CALIOP-based estimate of dust deposition into the Amazon Basin**

149   We calculate dust import to and export from the Amazon Basin in both zonal and

150   meridional directions. The divergence of dust import and export mass fluxes is attributed

151   to dust deposition into the Amazon Basin. **Figure 1** shows the budget of CALIOP best

152   estimate of seasonal dust transport (numbers in orange) and deposition (numbers in

153   white) into the Amazon Basin. The numbers represent the 7-year average ± 1 standard

154   deviation of the estimates. In boreal winter, dust import from zonal (eastern boundary)

155   and meridional (northern boundary) directions is 10.7±3.5 Tg and 4.4±1.2 Tg,

156   respectively. In boreal spring, the corresponding zonal and meridional import of dust is

157   13.8±3.2 Tg and 4.6±2.0 Tg, respectively. Clearly, the meridional mass flux entering the

158   Basin from the northern boundaries accounts for 33~41% of the zonal mass flux through

159   the eastern boundaries, and cannot be neglected. A large majority of the dust import (e.g.,

160   79~86%) is deposited in the Basin. The dust deposition in the Basin is 11.9±4.0 Tg and

161   15.8±3.0 Tg in DJF and MAM, respectively. On a basis of the 7-year average, the annual

162   dust deposition into the Amazon Basin amounts to 27.7 Tg a^{-1} (equivalent to 28.9 kg ha^{-1}

163   a^{-1}).

164

165   The multi-year CALIOP observations used in this study reveal interannual variation of

166   dust deposition into the Amazon Basin. **Figure 2a** shows the CALIOP-based best

167   estimate of dust deposition flux in DJF (blue bar) and MAM (red bar) in individual years.

168   The gray error bar indicates the range of DJF+MAM combined dust deposition estimates

169   introduced by uncertainty in separating dust from non-dust aerosol. It shows that the

170   year-to-year values can vary by as much as 29% of the 7-year mean. The dust deposition

171   in DJF and MAM, combined, ranges from 14.3 to 20.9 Tg and 33.6 to 43.2 Tg, for the

172   lower and upper bound, respectively. The figure also shows that the relative contribution

173   from DJF and MAM appears to be dependent on year.

174

175   The interannual variation of dust deposition is generally regulated by variations in

176   African dust emissions, atmospheric circulations, and rainfall along the dust transport

177   route *[Prospero and Lamb, 2003; Chin et al., 2014; Y15]. Y15* found that the annual

178   trans-Atlantic dust transport over the period of 2007-2013 has a statistically significant

179   anti-correlation with the prior-year wet-season rainfall anomaly in the Sahel or the so-

180   called Sahel Precipitation Index (SPI) *[Janowiak, 1988]*. Similarly we examined how the

181   annual dust transport and deposition into the Amazon Basin correlate with the prior-year

182   SPI, as shown in **Figure 2b**. Clearly the annual dust transport and deposition are anti-

183   correlated with the prior-year SPI, which is statistically significant at the 95% confidence

184   level. For the dust import to the Basin from the northern and eastern boundaries, the

185   value of R^2 (R is correlation coefficient) is 0.71. The dust deposition into the Basin and

186   export from the Basin show slightly weaker anti-correlation with SPI, with R^2 of 0.66 and

187   0.60, respectively. This may suggest that the variation of dust deposition into the Amazon

188   Basin is largely associated with that of prior-year Sahel rainfall condition.

189

190 The seasonal mean dust import to the Amazon Basin estimated from CALIOP

191 observations is correlated with surface PM_{10} measurements at Cayenne, French Guiana

192 (4.95°N, 52.31° W) during 2007-2011 *[Prospero et al., 2014]*, as shown in **Figure 2(c)**.

193 As discussed in *Prospero et al. [2014]*, the PM_{10} level at Cayenne is a good measure of

194 dust import into South America. The R^2 between CALIOP seasonal dust mass flux and

195 PM_{10} concentration is 0.65, which is statistically significant at the 95% confidence level.

196

197 In summary, on the basis of the 2007-2013 average, the CALIOP-based best estimate of

198 dust deposition into the Amazon Basin is 28 Tg a^{-1}, ranging from 8 to 48 Tg a^{-1} when

199 accounting for the estimated uncertainty of ±70% *[Y15]*. The interannual variation of

200 dust deposition is anti-correlated with the prior-year wet season Sahel rainfall. The

201 CALIOP-based estimate of dust import to the Amazon Basin is also well correlated with

202 surface aerosol measurements at Cayenne. In the following we further compare the

203 CALIOP-based estimate of dust deposition with simulation from the Goddard Chemistry

204 Aerosol Radiation and Transport (GOCART) model and other estimates in literature.

205

206 **3.2. Comparisons of CALIOP-based dust deposition estimate with models and other**

207 **observations**

208 The CALIOP-based estimate of dust deposition is compared with the GOCART model

209 simulation in the same region for 2007-2009. The GOCART is a global chemical

210 transport model that simulates major aerosol types including dust *[Chin et al., 2002]*. A

211 multi-decadal (1980-2009) run was performed at a horizontal resolution of 2° in latitude

212 by 2.5° in longitude *[Chin et al., 2014]*. In GOCART, the dust deposition to the surface is

213   calculated due to aerodynamic dry deposition, gravitational settling, and scavenging by

214   large-scale and convective clouds with parameterized schemes *[Chin et al., 2002]*. The

215   GOCART model suggests that wet removal accounts for about 86% of the total dust

216   deposition in the region during DJF and MAM. The GOCART model also reveals a high

217   heterogeneity of dust deposition in the Basin. The deposition north of 2°S accounts for

218   80~92 % of the total deposition in the Basin in DJF and MAM, because dust is injected

219   into the basin from the northeast coast of South America and precipitation is much

220   stronger in the northern part of the Basin than the southern part.

221

222   **Table 1** shows a comparison of the CALIOP-based estimates of seasonal dust deposition

223   with the GOCART model simulations during 2007-2009. On a seasonal basis the

224   GOCART-calculated dust deposition is 26~47 % lower than the best estimate from the

225   CALIOP observation. On the basis of the 3-year average, dust deposition for DJF and

226   MAM combined is 18.5 Tg from GOCART model, which is 35% lower than the

227   CALIOP 2007-2009 average of 28.3 Tg. However, the GOCART model also simulates a

228   dust deposition of 6.6 Tg in boreal summer and fall combined, when the CALIOP-

229   derived estimate of dust deposition is nearly 0.

230

231   A comparison of annual dust deposition between the CALIOP-based estimate and those

232   in the literature *[Swap et al., 1992; Ridley et al., 2012]* as well as GOCART *[Chin et al.,*

233   *2014]* and WRF-Chem *[Zhao et al., 2013]* simulations is summarized in **Table 2**. We

234   calculate the GOCART and WRF-Chem dust deposition into the same region as defined

235   in Figure 1. Apparently the CALIOP-based estimate of 28 (8~48) Tg falls in between the

236   MODIS-based estimate of 50 Tg *[Kaufman et al., 2005]* and those estimated from in situ

237   observations and model simulations (13~26 Tg). However, the apparent discrepancies

238   shown in the table should not be attributed to the uncertainties associated with individual

239   methods or data, because such a comparison is complicated by differences in regions and

240   years among the studies (see notes in the table).

241

242   We use the correlation between dust deposition and SPI (Figure 2b) to extrapolate the

243   CALIOP-derived values back to the same years as previous studies listed in Table 2. The

244   SPI value for 1986 (a year prior to the in situ observation in S92) and 2000 (a year prior

245   to the MODIS estimate in K05) is -2.04 and -1.25, respectively. Applying the regression

246   equation from Figure 2b, the dust deposition would have been 32 and 30 Tg in 1987 and

247   2001, respectively. These extrapolated values decrease the discrepancy between MODIS

248   and CALIOP by only 9% and increase the discrepancy between the in situ estimate and

249   CALIOP by 27%. Differences in years cannot explain the discrepancies in studies.

250

251   Can the definition of the Amazon Basin and the exclusion of meridional transport in K05

252   explain the discrepancy in dust deposition? The K05 estimate was made in a region of

253   [20°S-10°N, 35°W-75°W]. In contrast to that defined in Figure 1 and in other studies,

254   this region includes a portion of tropical Atlantic Ocean just off the northeastern coast of

255   South America where strong scavenging by intense rainfall could prevent a large amount

256   of dust from reaching the Amazon Basin. In addition, the MODIS estimate considered the

257   zonal transport of dust only, whereas other estimates accounted for both zonal and

258   meridional transport.

259

260   Here we use the CALIOP observations to estimate the dust deposition in the same region

261   as that used in K05. On a basis of the 7-year average applied to the K05 rectangular

262   domain, the CALIOP-derived net dust transport in the zonal direction alone is 49 Tg,

263   which is nearly the same as the K05 estimate of 50 Tg. We also found that the CALIOP-

264   derived meridional transport adds an additional 24 Tg of dust into the K05 domain. Thus

265   the total dust deposition, calculated from CALIOP, in the K05 domain amounts to 73 Tg,

266   which is 160% larger than the 28 Tg estimated for the domain defined in Figure 1. The

267   above practice underscores the importance of appropriately defining the Basin and

268   including the meridional transport. Improper assumptions, as per K05, will overestimate

269   the dust deposition, which could explain a significant portion of the discrepancies

270   documented in literature.

271

272   In summary, the CALIOP-based estimate of dust deposition shows a better agreement

273   with in situ measurements and model simulations than the MODIS-based estimate as

274   reported in literature. The closer agreement benefits from a more realistic geographic

275   definition of the Amazon Basin, and an inclusion of meridional dust transport, in addition

276   to the 3D nature of CALIOP measurements.

277

278   **3.3. Estimate of phosphorus input associated with African dust and implications for**

279   **Amazon rainforest**

280   Micronutrients such as phosphorus, carried by African dust can have important

281   implications for the biogeochemical cycle in the Amazon Basin. To estimate the amount

282   of phosphorous associated with the dust deposition of 28 (8~48) Tg a^{-1}, we must obtain

283   the mass concentration of phosphorus in the dust (C_{PD}). Observations at the Bodele

284   depression yielded a C_{PD} of 780 ppm *[Bristow et al., 2010]*, while those at Barbados and

285   Miami gave a higher C_{PD} of 880 ppm *[Zamora et al., 2013]*. *Mahowald et al. [2008]*

286   used C_{PD} of 720 ppm in their global model simulation. By using C_{PD} of 780 ppm, we

287   estimate that on the basis of a 7-year average, yearly total P deposition into the Amazon

288   Basin mounts to 0.022 (0.006~0.037) Tg P a^{-1} or equivalent to 23 (7~39) g P ha^{-1} a^{-1}.

289   Given that the dust deposition is highly heterogeneous, phosphorus-deposition should be

290   substantially higher in the central Amazon Basin where most of dust deposition is

291   expected. For comparison, S92 estimated a range of 11~47 g P ha^{-1} a^{-1} in a much smaller

292   study area of the central Amazon Basin. Note that our estimated P deposition is subjected

293   to uncertainty associated with C_{PD}. It is possible that C_{PD} may have changed during the

294   long-range transport. The issue could be investigated in the future by extracting dust and

295   associated P from accumulating aerosol measurements in the Amazon Basin *[Artaxo et*

296   *al., 2002]*.

297

298   How significant is the P input associated with African dust in the context of the

299   phosphorus cycle in the Basin? *Vitousek and Sanford [1986]* summarized that the

300   recycling of phosphorus through litterfalls is 1400~4100 g P ha^{-1} a^{-1} in the Amazon basin,

301   which is 61~178 fold of our best estimate of phosphorus input associated with dust

302   deposition. The total atmospheric deposition resulting from dust and non-dust sources

303   was estimated to be 161~300 g P ha^{-1} a^{-1} *[Vitousek and Sanford, 1986]*. Our estimated P

304   deposition associated with dust accounts for no more than 13% of the total atmospheric

305   deposition. Primarily biogenic aerosols and biomass burning smoke are thought to

306   contribute the remaining atmospheric phosphorus deposition *[Artaxo et al., 2002;*

307   *Mahowald et al., 2005].* Therefore the phosphorus associated with the dust is relatively

308   small as compared with the recycling and the deposition of biogenic and smoke particles.

309   On the other hand, our estimated phosphorus input associated with African dust is

310   comparable to the estimated hydrological loss of 8~40 g P ha^{-1} a^{-1} *[Vitousek and Sanford,*

311   *1986].* This suggests that African dust may have important implication for maintaining

312   the health of Amazon rainforests over the long term. Without the phosphorus input from

313   African dust, the hydrological loss would greatly deplete the soil phosphorus reservoir

314   over a time scale of decades or centuries and affect the health and productivity of the

315   Amazon rainforest.

316

317   Finally we would like to note that the amount of dust needed to provide adequate

318   phosphorus for maintaining the productivity of the Amazon rainforest remains unknown.

319   To quantify the amount, we require a much better understanding of all major components

320   of the phosphorus cycle (including the recycling through litterfalls, atmospheric

321   deposition of dust, smoke, and biological particles, and hydrological loss). Currently, our

322   knowledge does not warrant a claim with high level of confidence that there exists a

323   missing source of phosphorus for the Amazon Basin on the order of 50 Tg a^{-1} of African

324   dust as claimed by K05 or *[Ridley et al., 2012].*

325

326   **4.   Concluding remarks**

327 This study provides the first multiyear satellite-based estimate of dust deposition into the

328 Amazon Basin. We have estimated from the three-dimensional aerosol distribution

329 derived from the CALIOP 7-year (2007-2013) record that on average 28 (8~48) Tg a^{-1} or

330 29 (8~50) kg ha^{-1} a^{-1} of dust is deposited into the Amazon Basin during the wet season

331 (e.g., boreal winter and spring). On a seasonal basis, the estimated dust import to the

332 Amazon Basin is well correlated with surface aerosol measurements during 2007-2011 in

333 Cayenne, French Guiana. The dust deposition shows interannual variation of up to 29%,

334 which is negatively correlated with the prior year rainfall anomaly in the Sahel at the

335 95% confidence level.

336

337 The CALIOP-based multi-year mean estimate of dust deposition agrees better with

338 estimates from in-situ measurements and model simulations than the K05 MODIS-based

339 estimate does. The closer agreement benefits from a more realistic geographic definition

340 of the Amazon Basin and the inclusion of meridional dust transport, in addition to the 3D

341 nature of CALIOP aerosol measurements. These factors could explain a significant

342 portion of the large discrepancies between measurements and models as reported in

343 literature *[Swap et al., 1992; Kaufman et al., 2005; Ridley et al., 2012]*.

344

345 We further estimated that the phosphorus (P) input associated with the dust deposition is

346 0.022 (0.006~0.037) Tg P a^{-1} or 23 (7~39) g P ha^{-1}a^{-1}. Although this phosphorus-input

347 originating from outside the Basin is 1~2 order of magnitudes lower than the atmospheric

348 deposition of smoke and biological particles and the phosphorus recycling via litterfalls

349 within the Basin, it largely compensates the hydrological loss of phosphorus. This may

350   suggest an important role of African dust in preventing phosphorus depletion on time

351   scales of decades or centuries.

352

353

369

References

370 **References**

371 Ansmann, A., et al. (2009), Dust and smoke transport from Africa to South America:

372   Lidar profiling over Cape Verde and the Amazon rainforest, *Geophys. Res. Lett., 36,*

373   L11802, doi:10.1029/2009GL037923.

374 Artaxo, P., W. Maenhaut, H. Storms, and R. Van Grieken (1990), Aerosol characteristics

375   and sources for the Amazon Basin during the wet season, *J. Geophys. Res., 95,* 1605-

376   1615.

377 Artaxo, P., et al. (2002), Physical and chemical properties of aerosols in the wet and dry

378   seasons in Rondonia, Amazonia, *J. Geophys. Res., 107,* D20, 8081,

379   doi:10.1029/2001JD000666.

380 Baars, H., A. Ansmann, D. Althausen, R. Engelmann, P. Artaxo, T. Pauliquevis, and R.

381   Souza (2011), Further evidence for significant smoke transport from Africa to

382   Amazonia, *Geophys. Res. Lett., 38,* L20802, doi:10.1029/2011GL049200.

383 Baars, H., et al. (2012), Aerosol profiling with lidar in the Amazon Basin during the wet

384   and dry seasons, *J. Geophys. Res., 117,* D21201, 10.1029/2012JD018338.

385 Ben-Ami, Y., Y. Koren, Y. Rudich, P. Artaxo, S. T. martin, and M. O. Andreae,

386   Transport of North African dust from the Bodele depression to the Amazon Basin: a

387   case study, *Atmos. Chem. Phys., 10,* 7533-7544, 2010.

388 Bristow, C. S., K. A. Hudson-Edwards, and A. Chappell (2010), Fertilizing the Amazon

389   and equatorial Atlantic with West African dust, *Geophys. Res. Lett., 37,* L14807,

390   doi:10.1029/2010GL043486.

391 Chin, M., P. Ginoux, S. Kinne, O. Torres, B. N. Holben, B. N. Duncan, R. V. Martin, J.

392   A. Logan, A. Higurashi, and T. Nakajima (2002), Tropospheric aerosol optical

393   thickness from the GOCART model and comparisons with satellite and sunphotometer

394   measurements, *J. Atmos. Sci., 59,* 461-483.

395 Chin, M., et al. (2014), Multi-decadal aerosol variations from 1980 to 2009: a perspective

396   from observations and a global model, *Atmos. Chem. Phys., 14,* 3657-3690.

397 Formenti, P., et al. (2001), Saharan dust in Brazil and Suriname during the Large-Scale

398   Biosphere-Atmosphere Experiment in Amazonia (LBA) – Cooperative LBA Regional

399   Experiment (CLAIRE) in March 1998, *J. Geophys. Res., 106,* 14919-14934.

400

401 Janowiak, J. E. (1988), An investigation of interannual rainfall variability in Africa. *J.*
402   *Climate, 1,* 240-255.

403 Kaufman, Y. J., I. Koren, L. A. Remer, D. Tanré, P. Ginoux, and S. Fan (2005), Dust
404   transport and deposition observed from the Terra-Moderate Resolution Imaging
405   Spectroradiometer (MODIS) spacecraft over the Atlantic Ocean, *J. Geophys. Res.,*
406   *110,* D10S12, doi:10.1029/2003JD004436.

407 Liu, Z., D. Winker, A. Omar, M. Vaughan, J. Kar, C. Trepte, Y. Hu, and G. Schuster
408   (2014), Evaluation of CALIOP 532 nm AOD over opaque water clouds, *Atmos. Chem.*
409   *Phys. Discuss., 14,* 23583-23637.

410 Mahowald, N. M., P. Artaxo, A. R. Baker, T. D. Jickells, G. S. Okin, J. T. Randerson,
411   and A. R. Townsend (2005), Impacts of biomass burning emissions and land use
412   change on Amazonian atmospheric phosphorous cycling and deposition, Global
413   Biogeochem. Cycle, 19, GB4030, doi:10.1029/2005GB002541.

414 Mahowald, N., et al. (2008), Global distribution of atmospheric phosphorus sources,
415   concentrations and deposition rates, and anthropogenic impacts, *Global Biogeochem.*
416   *Cycles, 22,* GB4026, doi:10.1029/2008GB003240.

417 Malhi, Y., J. T. Roberts, R. A. Betts, T. J. Killeen, W. Li, and C. A. Nobre (2008),
418   Climate change, deforestation, and the fate of the Amazon, *Science, 319*, 169-172.

419 Mercado L. M., et al. (2011) Variations in Amazon forest productivity correlated with
420   foliar nutrients and modeled rates of photosynthetic carbon supply. *Phil. Trans. R.*
421   *Soc. B 366,* 3316–3329. doi:10.1098/rstb.2011.0045.

422 Nepstad, D. C., C. M. Stickler, B. S. Filho, and F. Merry (2008), Interactions among
423   Amazon land use, forests and climate: Prospects for a near-term forest tipping point.
424   *Philos Trans R Soc Lond B Biol Sci., 363(1498),*1737–1746.

425 Okin, G. S., N. Mahowald, O. A. Chadwick, and P. Artaxo (2004), Impact of desert dust
426   on the biogeochemistry of phosphorus in terrestrial ecosystem, *Global Biogeochem.*
427   *Cycles, 18,* GB2005, doi:10.1029/2003GB002145.

428 Prospero, J. M., et al. (1981), Atmospheric transport of soil dust from Africa to South-
429   America, *Nature, 289,* 570–572, doi:10.1038/289570a0.

430 Prospero, J. M. and P. J. Lamb (2003), African droughts and dust transport to the
431   Caribbean: climate change implications, *Science, 302,* 1024–1027.

432 Prospero, J. M., F.-X. Collard, J. Molinie, and A. Jeannot (2014), Characterizing the

433   annual cycle of African dust transport to the Caribbean Basin and South America and

434   its impact on air quality and the environment, *Global Biogeochem. Cycles, 29,* 757–

435   773, doi:10.1002/2013GB004802.

436 Ridley, D. A., C. L. Heald, and B. Ford (2012), North African dust export and deposition:

437   A satellite and model perspective, *J. Geophys. Res., 117,* D02202,

438   doi:10.1029/2011JD016794.

439 Sanchez, P. A., D. E. Bandy, J. H. Villachica, and J. J. Nicholaides (1982), Amazon basin

440   soils: Management for continuous crop production, *Science, 216,* 821-827.

441 Schafer, J. S., T. F. Eck, B. N. Holben, P. Artaxo, and F. Duarte (2008), Characterization

442   of the optical properties of atmospheric aerosols in Amazonia from long-term

443   AERONET monitoring (1993-1995 and 1999-2006), *J. Geophys. Res., 113,* 1-16,

444   doi:10.1029/2007JD009319.

445 Shukla, J., C. Nobre, and P. Sellers (1990), Amazon deforestation and climate change,

446   *Science, 247,* 1322-1325.

447 Swap, R., M. Garstang, S. Greco, R. Talbot, and P. Kållberg (1992), Saharan dust in the

448   Amazon Basin, *Tellus, Ser. B, 44,* 133–149, doi:10.1034/j.1600-0889.1992.t01-1-

449   00005.x.

450 Talbot, R. W., M. O. Andreae, H. Berresheim, P. Artaxo, M. Garstang, R. C. Harris, K.

451   M. Beecher, and S. M. Li, (1990), Aerosol chemistry during the wet season in central

452   Amazonia: the influence of long-range transport, *J. Geophys. Res., 95,* 16955-16969.

453 Vitousek, P. M. (1984), Litterfall, nutrient cycling, and nutrient limitation in tropical

454   forests*, Ecology, 65,* 285–298. doi:10.2307/1939481.

455 Vitousek, P. M., and R. L. Sanford (1986), Nutrient cycling in moist tropical forest, *Ann.*

456   *Rev. Ecol. Syst., 17,* 137-167.

457 Winker, D. M., J. L. Tackett, B. J. Getzewich, Z. Liu, M. A. Vaughan, and R. R. Rogers

458   (2013), The global 3-D distribution of tropospheric aerosols as characterized by

459   CALIOP, *Atmos. Chem. Phys., 13,* 3345-3361, doi:10.5194/acp-13-3345-2013.

460 Yu H., L. A. Remer, M. Chin, H. Bian, R. G. Kleidman, and T. Diehl (2008), A satellite-

461   based assessment of transpacific transport of pollution aerosol, *J. Geophys. Res., 113,*

462   D14S12, doi:10.1029/2007JD009349.

463   Yu, H., L. A. Remer, M. Chin, H. Bian, Q. Tan, T. Yuan, and Y. Zhang (2012a),

464   Aerosols from overseas rival domestic emissions over North America, *Science, 337,*

465   566-569, doi:10.1126/science.1217576.

466   Yu, H., Y. Zhang, M. Chin, Z. Liu, A. Omar, L.A. Remer, Y. Yang, T. Yuan, and J.

467   Zhang (2012b). An integrated analysis of aerosol above clouds from A-Train multi-

468   sensor measurements, *Rem. Sens. Environ, 121*, 125-131,

469   doi:10.1016/j.rse.2012.01.011.

470   Yu, H., L. A. Remer, R. A. Kahn, M. Chin, and Y. Zhang (2013), Satellite perspective of

471   aerosol intercontinental transport: from qualitative tracking to quantitative

472   characterization, *Atmos. Res.*, 124, 73-100, doi:10.1016/j.atmosres.2012.12.013.

473   Yu, H., and Z. Zhang (2013), New Directions: Emerging satellite observations of above-

474   cloud aerosols and direct radiative forcing, *Atmos. Environ.*, 72, 36-40,

475   doi:10.1016/j.atmosenv.2013.02.17.

476   Yu, H. M. Chin, H. Bian, T. Yuan, J. M. Prospero, A. H. Omar, L. A. Remer, D. M.

477   Winker, Y. Yang, Y. Zhang, and Z. Zhang (2015), Quantification of trans-Atlantic

478   dust transport from seven-year (2007-2013) record of CALIPSO lidar measurements,

479   *Remote Sens. Environ., http://dx.doi.org/10.1016/j.rse.2014.12.010, in press.*

480   Zamora, L.M., J. M. Prospero, D. A. Hansell, and J. M. Trapp (2013), Atmospheric P

481   deposition to the subtropical North Atlantic: sources, properties, and relationship to N

482   deposition, *J. Geophys. Res. Atmos., 118,* 1546-1562, doi:10.1002/jgrd.50187.

483   Zhao, C., S. Chen, L. R. Leung, Y. Qian, J. F. Kok, R. A. Zaveri, and J. Huang (2013),

484   Uncertainty in modeling dust mass balance and radiative forcing from size

485   parameterization, *Atmos. Chem. Phys., 13,* 10733-10753.

486

488 **Figure Captions**

489

490 **Figure 1**: CALIOP estimated seasonal dust mass fluxes (orange color, mean ± 1σ, σ

491 represents the standard deviation over the 7 years) across the boundaries of the Amazon

492 Basin (red lines) and the estimated dust deposition (white color) in the Basin: (a) DJF,

493 and (b) MAM. All numbers have a unit of Tg. The background shows MODIS enhanced

494 vegetation index, with the shade of green indicating the density of vegetation (dark for

495 high density and light for low density).

496

497 **Figure 2:** (a) CALIOP estimates of dust deposition (Tg) into the Amazon Basin. The

498 wide stacked color (blue for DJF and red for MAM) bars represent mean dust deposition,

499 while error bars indicate the lower bound and upper bound of DJF+MAM combined dust

500 deposition associated with the dust discrimination schemes. On a basis of a 7-year

501 average, the best estimate of dust deposition into the Amazon Basin amounts to 28 Tg for

502 DJF and MAM combined. (b) Correlation of CALIOP-estimated DJF+MAM total dust

503 import to, export from, and deposition into the Amazon Basin with prior-year Sahel

504 Precipitation Index (SPI). (c) Correlation of CALIOP estimated seasonal dust mass flux

505 in zonal direction into the Amazon Basin with PM_{10} concentration measured at Cayenne,

506 French Guiana over the period of 2007-2011.
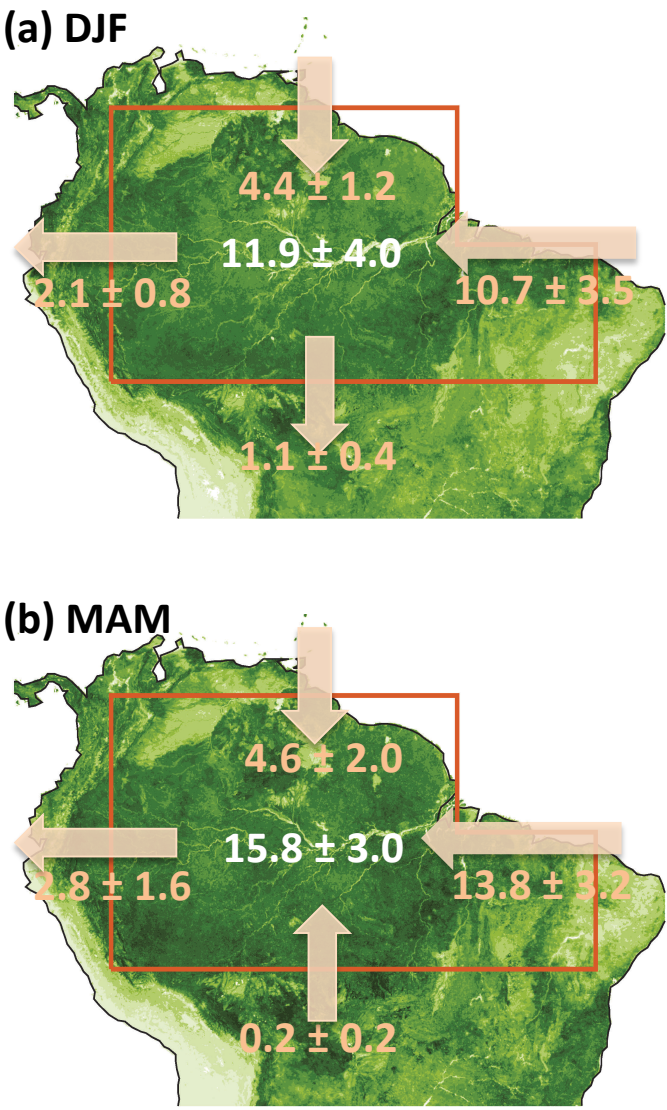
507

508

509

Table 1: Comparison of GOCART simulated dust deposition (Tg) into the Amazon Basin (white-solid boundaries in Figure 1a) with the CALIOP-based best estimate of dust deposition. Shown in parentheses is the range of CALIOP estimates bounded by the dust discrimination scenarios.								
Year	2007		2008		2009		2007-2009 average	
Season	DJF	MAM	DJF	MAM	DJF	MAM	DJF	MAM
CALIOP	18.0 (11.2-24.8)	14.0 (9.7-18.4)	12.7 (7.6-17.8)	15.6 (10.5-20.7)	9.1 (5.0-13.2)	15.2 (9.3-21.2)	13.3 (7.9-18.6)	15.0 (8.9-20.1)
GOCART	12.6	10.4	7.3	10.9	4.8	9.6	8.2	10.3

510
511

512

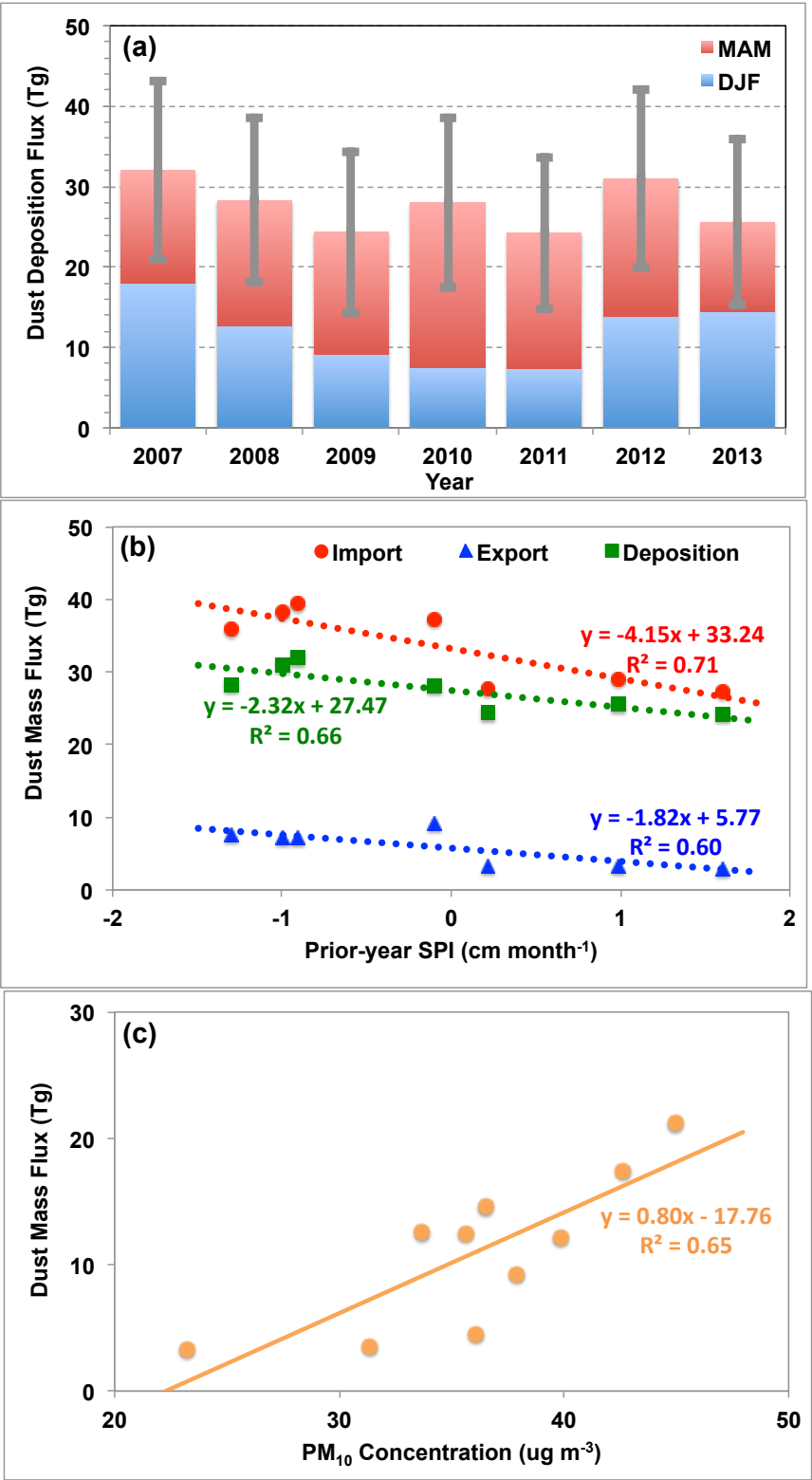|				
Table 2: Summary of comparisons of CALIOP-based estimates of annual dust deposition into the Amazon Basin with those in the literature.				
Source	Total dust deposition (Tg)	Dust deposition per area (kg ha^{-1})	Averaging region and years	References
CALIOP	28 (8 ~ 48)	29 (8 ~ 50)	see Figure 1 for the defined region; 2007-2013 average	*This study*
MODIS	50	n/a	[20°S-10°N, 35°W-75°W]; 2001	*Kaufman et al. [2005]*
In-situ observations	13 (9 ~ 19)	190	Assuming all the imported dust is deposited in a small area of Central Amazon Basin; 1987	*Swap et al. [1992]*
GOCART model	26	27	same region as the CALIOP estimate; 1980-2009 average	*This study; Chin et al. [2014]*
WRF-Chem model	19	20	same region as the CALIOP estimate; 2011-2013 average	*This study; Zhao et al. [2013]*
GEOS-Chem model	17	n/a	10°S-10°N land only (similar to the CALIOP estimate), 2006-2008 average	*Ridley et al. [2012]*

513

514

(a) DJF

4.4 ± 1.2

11.9 ± 4.0

2.1 ± 0.8   10.7 ± 3.5

1.1 ± 0.4

(b) MAM

4.6 ± 2.0

15.8 ± 3.0

2.8 ± 1.6   13.8 ± 3.2

0.2 ± 0.2

515

Figure 1

517

518
519 **Figure 2**
520